ASACUSA Gas-Jet Target: Present Status And Future Development

V.L. Varentsov[2, 3], N. Kuroda [2], Y. Nagata [1, 2], H. A. Torii [1], M. Shibata[2], Y. Yamazaki[1, 2]

[1]*Institute of Physics, University of Tokyo, Komaba, Meguro-ku,Tokyo 153-8902, Japan*
[2]*Atomic Physics Laboratory, RIKEN, Wako, Saitama 351-0198, Japan*
[3]*V.G. Khlopin Radium Institute, 2nd Murinskiy Ave. 28, 194021, St. Petersburg, Russia*

Abstract. A supersonic gas-jet target apparatus that have been prepared to study elementary processes of antiprotonic atoms formation using monoenergetic ultra-slow antiproton beams is described. We investigated an operation of this target with cryogenically cooled nozzle by both gas dynamic simulations and supersonic jet measurements. In result, the helium target density of $2 \cdot 10^{12}$ atoms/cm^3 has been obtained.

For considerable increasing of the target density, a qualitative modification of the present target setup is suggested. The goal can be achieved by the use of pulsed high-pressure supersonic gas jet that operates in accordance with the pulsed mode of the MUSASHI penning trap. For this purpose an additional stage of differential pumping with a skimmer will be set into the present target setup. To avoid the clusters in the gas-jet target, a sonic nozzle equipped with a solenoid driven pulsed gas valve will be used at room or higher temperatures. The operation of this future version of the gas-jet target apparatus has been studied by means of detailed computer simulations. Results of these calculations for helium, which show the possibility of pulsed gas target production of $3 \cdot 10^{13}$ atoms/cm^3 density· are presented also.

INTRODUCTION

Antiproton, the antiparticle counterpart of the proton is an exotic but interesting probe for atomic physic. Now that antiprotons can be prepared as a monoenergetic beam at electronvolt energies from the ASACUSA-MUSASHI apparatus [1], the next natural step is to study collision dynamics including ionization of atoms by antiproton impact and capture of an antiproton to form an antiprotonic atom. Formation processes of antiprotonic atoms can be studied by employing collisions between an ultra-slow antiproton beam and a thin gas target *A* under single collision conditions:

$$\overline{p} + A \rightarrow \overline{p}A^+ + e^-$$
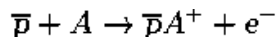
at an energy comparable to the ionization potential of the target atom. Atomic formation and ionization processes will be detected by taking coincidence between signals of antiproton annihilation and the electron released from the target atom.

Since the number of antiprotons available as ultra-slow beams is very much limited, the reaction probability must be maximized in order to make best use of the

antiprotons, and therefore a maximum possible density of atomic gas jets need to be prepared to be crossed with the antiprotonic beams. The number of antiprotonic atoms formed is given by the formula

$$N_{\overline{p}A^+} = \sigma\, n_A\, L\, N_{\overline{p}},$$

where $N_{\overline{p}A}$ is the number of the antiprotonic atoms, σ is the formation cross section, n_A is the number density of the atomic target, L is the interaction length, and $N_{\overline{p}}$ is the number of antiprotons.

Atomic formation cross sections are naturally of the order of 10^{-16} cm^2, as was confirmed by a few theoretical calculations [2]. Suppose a beam with 10^5 antiprotons is available every shot per several minutes [1], we will obtain 10^2 antiprotonic atoms for a gas density of 10^{13} atoms/cm^3 at an interaction length of 1 cm. This number is almost at the lower limit of detection in order to assure enough statistical significance for the formation events to be distinguished from background events. At our early stage of development, several ideas for realization of an atomic-beam target were considered [3]. Usage of effusive gas out of micro-capillary array was also considered, but was rejected in favor of supersonic gas jets with a cryo-cold head for two main reasons: 1) the gas flow should be well-collimated and 2) the background vacuum in a collision chamber should be kept at a level below 10^{-6} Torr to allow operation of multichannel plate (MCP) for particle detection and to ensure an ultra-high vacuum of 10^{-12} Torr in the antiproton trap 3 m upstream by differential pumping with three apertures in the antiproton beamline [4].

To begin with, we will prepare rare gas atomic targets starting with the simplest helium atom, before we shall consider atomic and molecular hydrogen targets, which are though simple from theoretical point of view, confront experimental difficulties including special safety precautions needed to be taken.

EXPERIMENTAL SETUP

A schematic figure of the present ASACUSA gas-jet target setup is presented in Fig. 1. It has five differentially pumped vacuum chambers, which are evacuated by turbo molecular pumps (TMP). The first chamber, where the supersonic jet expands into vacuum, is evacuated by a large TMP (Pfeiffer TPH2101P), and backed by a rotary vane pump (Alcatel, 63 m^3/h). An effective pumping speed of this chamber consists of 1076 l/s for helium, when a gas flow rate through the nozzle is 6.6 mbar l/s. Through the conical skimmer the expansion chamber communicates with the next chamber that is pumped by two TMP (Pfeiffer TMH261), each having a nominal pumping speed for helium of 220 l/s, backed by one rotary vane pump (Alcatel 33 m^3/h). The third chamber, where the ultra slow antiproton beam crosses the target-beam and a detector system is placed, provides an additional stage of differential pumping. This collision chamber, communicating with the second chamber by means of a collimator, is pumped by TMP (Leybold TURBOVAC600), and backed by a rotary vane pump (Alcatel, 15 m^3/h). The last two differentially pumping stages are provided by target-beam dump chambers, which are communicate with each other and

the collision chamber by means of short rectangular tubes which are used as diaphragms. The first of these chambers is pumped by TMP (Leybold TURBOVAC600), backed by a rotary vane pump (Alcatel, 15 m^3/h). The other one is evacuated by a large TMP (Pfeiffer TPH2101P), backed by a rotary vane pump (Alcatel, 33 m^3/h). The effective pumping speeds and background gas pressures under typical gas-jet operation conditions are shown in the Fig. 1.
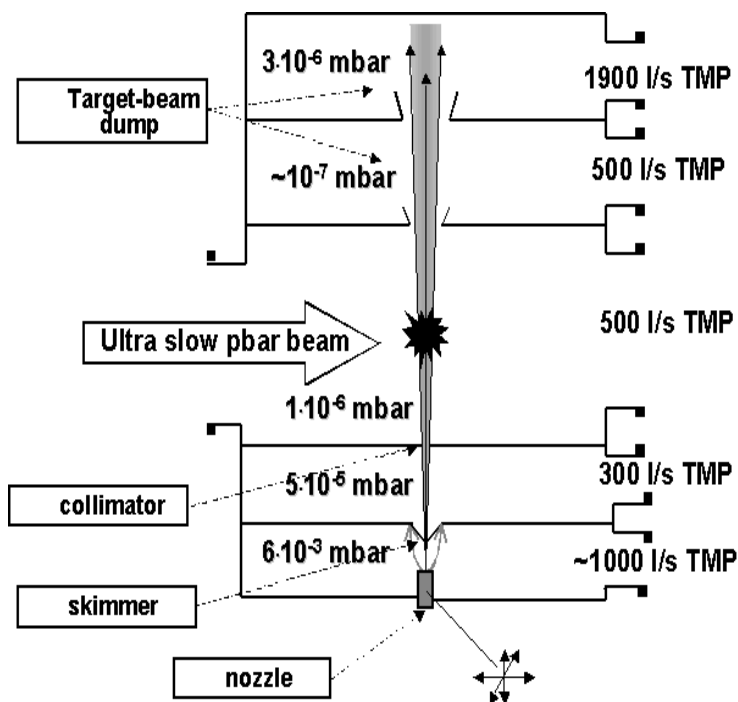

FIGURE 1. Schematic figure of the present gas-jet target setup. Five differentially pumped vacuum chambers are evacuated by turbo molecular pumps (TMP). The effective pumping speeds and background gas pressures under typical helium gas-jet operation conditions are shown.

The supersonic jet is produced by gas expansion into vacuum through the nozzle (in our case it is a hole of 0.1 mm in diameter in a gas cell wall). The gas cell with the nozzle is mounted on a cryogenically cooled head that allows decreasing a gas stagnation temperature (in the gas cell) down to 30 K. The cryogenic head, in its turn, is mounted on a movable base that can be displaced under vacuum along the three perpendicular x-y-z axes by means of two bellows. This x-y-z movement of the nozzle allows getting an alignment of the supersonic gas jet relatively to the fixed skimmer-collimator axis and regulating the nozzle-skimmer distance. We used it also for the jet profiles measurements, which are described in the next section.

The skimmer cuts out the small axial part of the supersonic jet with the forming of the target-beam. In order to minimize the gas flow perturbations at the skimmer entrance, a high quality and precision commercial one (Beam Dynamic Inc., model 10.2) is used. It has a parabolic profile, ultra-thin walls and ultra-sharp orifice edges. The skimmer is mounted on a removable supporting flange and has an entrance orifice diameter of 0.6 mm.

For final target-beam formation, a thin rectangular-shape collimator is used. The collimator has 2.2x4.4 mm aperture and is placed at 35 mm distance from the skimmer entrance.

The shape and sizes of the target-beam in the collision chamber at 50 mm distance from the collimator, where it crosses the antiproton beam, is determined by the described skimmer-collimator geometry. So, the target has 10 mm length at the antiproton beam direction and 5 mm length at the perpendicular one. It should be noticed that such rectangular target-beam geometry has an advantage over a circular beam of 10 mm diameter. Target thickness (it is a product of target density and length in the beam direction) for both cases is near the same. But, taking into account that a 5 mm target size at the perpendicular direction is enough to overlap the antiproton beam, the described rectangular target-beam shape allows improvement of vacuum in the collision chamber due to the decreasing of the gas load into the collision chamber and increasing, at the same time, the operation efficiency of the target-beam dump system.

The distances from the antiproton beam axis to entrances into the 1st and 2nd target-beam dump chambers are 50 mm and 100mm, correspondingly. The diaphragm of the 1st dump chamber has 23.3x11.7 mm aperture with a tube length at the target-beam direction of 15 mm, the 2nd one has 31.7x15.9 mm aperture with the tube length of 25 mm. The length of the 2nd dump chamber at the target-beam direction is 80 mm.

SUPERSONIC JET MEASUREMENTS AND SIMULATIONS

The operation of the described supersonic gas-jet target apparatus has been investigated in supersonic jet measurements and gas dynamic simulations. The supersonic jet profiles were measured with an impact pressure probe (often called a Pitot tube), which design is presented in Fig.2.
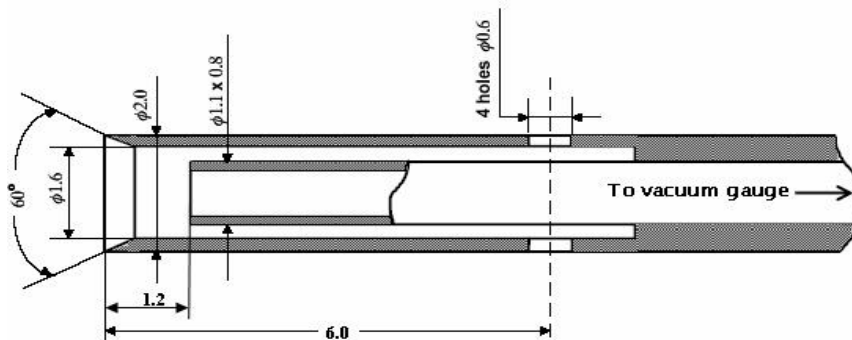

FIGURE 2. Schematic of the Pitot tube design.

The Pitot tubes of this design (Fig.2) have been used first in old experiments at LNPI [5] (Russia), then at GSI [6], LMU-Munich [7] (Germany) and NSCL-MSU [8] (USA). Such a Pitot tube consists of two coaxial combined tubes with 4 small holes drilled in the outer tube wall (see Fig.2). The Pitot tube of this design has an advantage over a simple Pitot tubes because it is insensitive to an angle between Pitot tube axis and an impact gas flow direction. It provides for measurements with accuracy better than 1% up to the angle of 20 degree even at high Mach numbers in the jet [9]. It is interesting to note that a simple tube of 1.02 mm outer diameter has been used in [10] to determine the gas flow angle to the axis in the supersonic nozzle and a low-density nitrogen supersonic jet. In our jet profiles measurements the skimmer was replaced by the Pitot tube (mounted on the holding flange) exactly at the position of the skimmer entrance orifice. In order to determine an optimum stagnation condition (temperature T_0 and pressure P_0) and a corresponding nozzle-skimmer distance, at which the greatest possible target density is achieved, measurements of the total gas flow rates through the collimator have been carried out also.

Potentialities of the present gas-jet target setup have been also investigated in computer simulations with the VARJET gas dynamic code based on a solution of full time-dependent system of Navier-Stokes equations. This code is described in details in [11], where results of computer experiments for generation of various internal molecular and atomic beam targets from gases and nonvolatile substances are presented as well.

Some results of our Pitot pressure measurements and corresponding calculations for the nozzle temperature $T_0 = 300$ K and stagnation pressure $P_0 = 2$ bar are shown in the Fig. 3. Large disagreement between measurement and calculation at 2 mm distance from the nozzle in Fig.3a may be explained by proximity of the Pitot tube of 2 mm diameter to the nozzle (e.g. the Pitot tube can change local pumping conditions due to its relatively big size). There is some disagreement also between measurements and calculations in description of a radial supersonic jet shape (Fig.3b). The reason has to do with a design defect of our present manipulator for the nozzle movement in x-y directions (perpendicular to the skimmer-collimator axis), because the bellows, which are used to enable the nozzle movement in vacuum, have a resistance force for the x-y movement. It is apparent from an asymmetry of the experimental jet profile in the Fig.3b, because it is obvious that the gas flow from a circular nozzle should be cylindrically symmetric.

In result of investigation of the present target setup operation we have found that the maximum helium target density is achieved when the stagnation pressure $P_0 = 1.4$ bar at the nozzle temperature $T_0 = 150$ K. Figure 4 shows results of measurements of the helium target density as a function of the nozzle-skimmer distance.

The target density n (in atoms/cm^3) can be obtained from measurements of total gas flow $\Phi_{tot} = \Phi_3 + \Phi_4 + \Phi_5$ (in mbar·l/s) through the collimator absorbed by the pump of collision chamber Φ_3 (when it is disconnected by flange from the pbar beam line) and Φ_4 and Φ_5 evacuated by pumps of two target-beam dump chambers. The gas flow Φ_i is equal to a product of the pressure increase ΔP_i in the vacuum chamber in response to the jet flow from the nozzle (measured by vacuum gauge) and known

pumping speed S_i (in l/s): $\Phi_i = \Delta P_i \cdot S_i$. Notice, that at room temperature 1 mbar·l/s = $2.4 \cdot 10^{19}$ atoms/s.

(a)

(b)

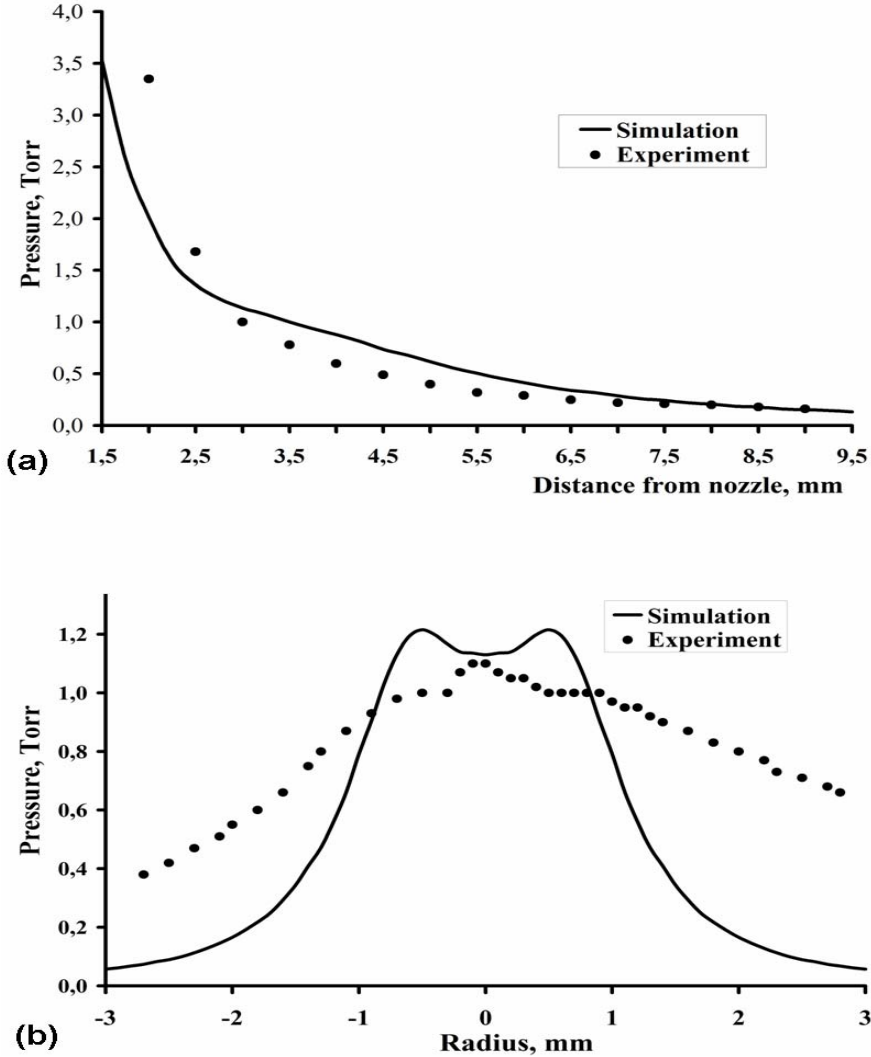**FIGURE 3.** The Pitot pressure profiles of the helium supersonic jet for the nozzle temperature $T_0 = 300$ K and stagnation pressure $P_0 = 2$ bar. (a) The pressure along the axis. (b) The radial pressure distribution at 3 mm downstream the nozzle.

To determine the target density, one can use the following equation $n = \Phi_{tot} / (A_b V_b)$, where A_b is area of a target-beam cross section (in cm²) and V_b is value of an atomic beam velocity (in cm/s). The target-beam area A_b is defined only by the skimmer-collimator geometry and in our case it is about 0.5 cm². The beam velocity

V_b is equal to the gas jet velocity V_{jet} at the skimmer entrance. The V_{jet} for big Mach numbers can be estimated in the isentropic approximation using the following equation:

$$V_{jet} = \sqrt{\frac{2\gamma k T_0}{m(\gamma - 1)}} \ ,$$

where γ is the ratio of specific heats, k is Boltzmann's constant and m is atomic mass.

The V_{jet} can be obtained with a good accuracy for any Mach number from our VARJET simulations as well. E.g. the described method of the target density measurement has been used in works [12-14] as well.
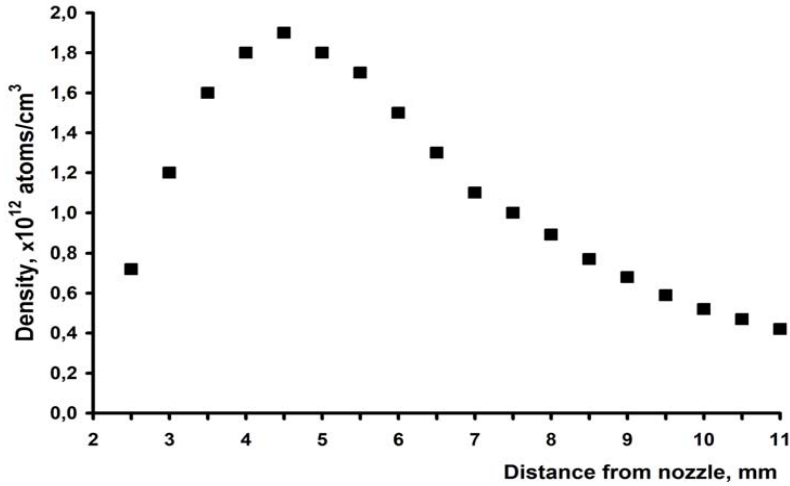

FIGURE 4. The helium target density as a function of the nozzle-skimmer distance for the nozzle temperature $T_0 = 150$ K and the stagnation pressure $P_0 = 1.4$ bar.

It can be seen that a target density curve has a maximum when the skimmer is placed at 4-5 mm distance from the nozzle. It is a matter of common knowledge that for an optimum skimmer position, a Knudsen number determined as a ratio of a free pass length to the skimmer orifice diameter should be about one. According to our simulation for $T_0 = 150$ K and $P_0 = 1.4$ bar, the helium density on the axis of supersonic jet at 4 mm downstream the nozzle is $5.7 \cdot 10^{15}$ atoms/cm³. So, the Knudsen number, in this instance, for the skimmer diameter of 0.6 mm is about 1.1.

Some results of computer simulations for the present gas-jet target setup are listed in the Table 1.

TABLE1. Main characteristics of He supersonic gas-jet target for the present target setup

Nozzle diameter	0.1 mm
Skimmer diameter	0.6 mm
Collimator	2.2x4.4 mm
Collimator-skimmer distance	35 mm
Nozzle-skimmer distance	4 mm
Stagnation temperature	150 K
Stagnation pressure	1.4 bar
Gas flow rate through the nozzle	6.6 mbar·l/s
Beam temperature	13.1 K
Mach number	5.9
Beam velocity	1190 m/s
Target cross section	5 x 10 mm
Target-beam density	$1.8 \cdot 10^{12}$ atoms/cm^3

As evident from Tab. 1, the calculated helium target density is in a good agreement with the experimental one.

It should be pointed out that, in principle, the decreasing of stagnation temperature at constant value of the total gas flow rate through the nozzle makes possible higher Mach numbers in the jet and thus higher gas target densities. The reason is that gas viscosity effects decrease with temperature decreasing. So, our simulation for 6.6 mbar·l/s the helium flow rate through the nozzle of 0.1 mm throat diameter and stagnation temperature T_0 = 30 K revealed that the target density may be as much as $1 \cdot 10^{13}$ atoms/cm^3 even for the present gas-jet target apparatus. Unfortunately, due to some design defect of the present setup, a tilting of the cryogenic head (with the nozzle) about skimmer-collimator axis takes place on cooling, causing the target density to decrease.

ASACUSA TARGET FUTURE DEVELOPMENT

For considerable increasing of the ASACUSA gas-jet target density, a qualitative modification of the present target setup is scheduled for future experiments with ultra slow antiprotons. The goal can be achieved by the use of pulsed high-pressure supersonic gas jet that operates in accordance with the pulsed mode of the MUSASHI penning trap [15]. For this purpose an additional stage of differential pumping with a skimmer will be set into the present target setup. To avoid the clusters in gas-jet targets of different gases, the nozzle will operate at room or higher temperatures.

Typical ultra slow antiproton beam pulse duration is about 10 s with a repetition rate of 0.01 Hz (one antiproton shot per 100 s). So, the using of pulsed mode of supersonic gas jet from a converging sonic nozzle equipped with a solenoid driven pulsed gas valve will allow using much higher stagnation pressures keeping the same level of time-average gas consumption. The operation of the pulsed nozzles for producing molecular and cluster beams have been described elsewhere [16-21].

The using of higher stagnation pressures provides a way of achieving larger Mach numbers in the jet and, as a result, obtaining higher target densities.

Schematic figure of a future gas-jet target setup is presented in Fig. 5. The distance between skimmers is 25 mm. The higher stagnation pressure P_0 in the nozzle leads to increase of background gas pressure in the nozzle exhaust chamber, so that this background pressure during the helium jet-pulse from the nozzle of 0.1 mm throat diameter at P_0 = 23 bar will be about 0.1 mbar. That's why we will need to use a Roots pump of about 800 l/s (see Fig.5) instead of presently used turbo molecular pump (Pfeiffer TMH261).
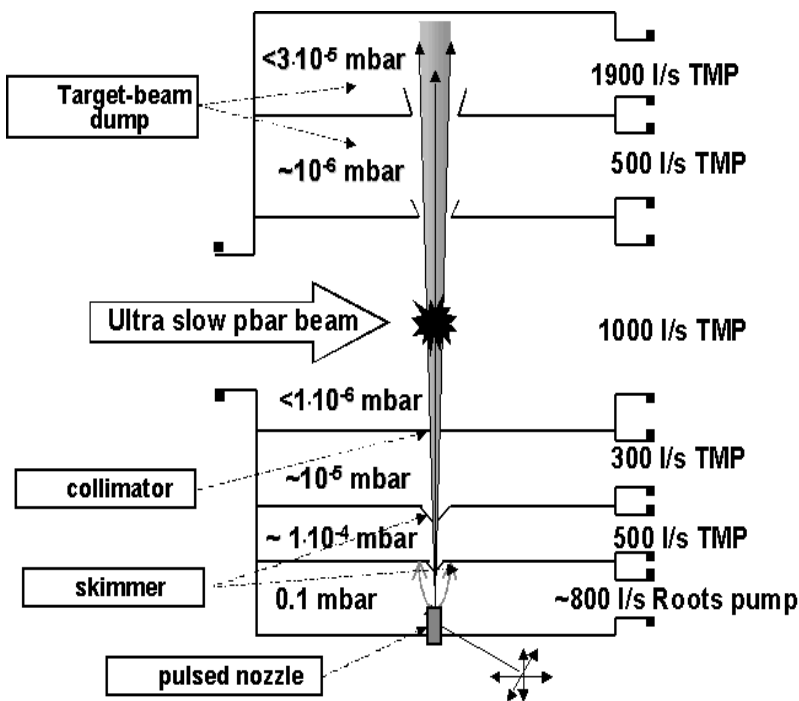

FIGURE 5. Schematic figure of a future gas-jet target setup. The sonic nozzle is equipped with a solenoid driven pulsed gas valve. Given pressure values show typical vacuum conditions in the system during the helium jet-pulse.

The operation of the described future version of the ASACUSA gas-jet target apparatus has been studied by means of detailed time-dependent simulations with VARJET code [11]. Among other things the simulations revealed that a steady flow of the He supersonic jet is attained within 1 ms after the pulsed gas valve opening. So, to ensure that the gas target density remain constant throughout an antiproton beam shot, all one only has to do is to open the gas valve 1 ms before the first antiproton from MUSHASHI penning trap will reach the target position in the collision chamber. By way of illustration, Fig. 6 shows calculated time profile of the axial He jet velocity at 11 mm downstream the nozzle.
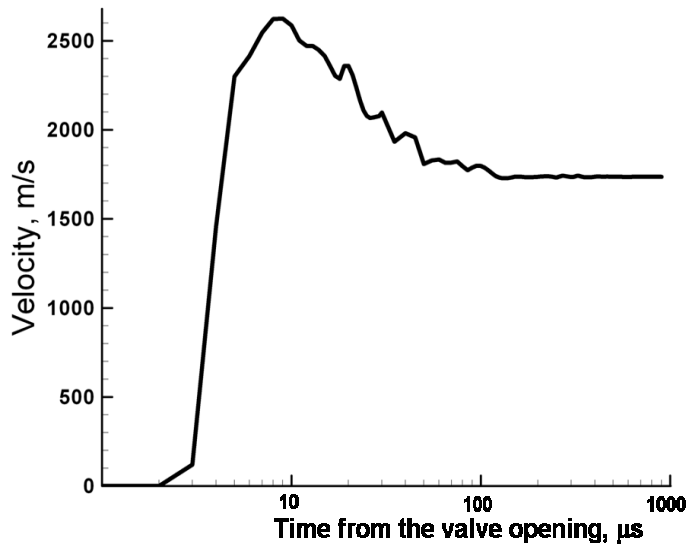
FIGURE 6. Calculated time profile of the axial He jet velocity at 11 mm downstream the nozzle for $P_0 = 22.6$ bar, $T_0 = 300$ K. The nozzle throat diameter is 0.1 mm.

Some results of these calculations for pulsed He gas-jet target are presented in Figs. 7 and 8. Figure 7 shows the static pressure, density, Mach number and static temperature distributions along the axis of He pulsed jet for $P_0 = 22.6$ bar, $T_0 = 300$ K. The converging sonic nozzle throat diameter is 0.1 mm. The helium density on the jet axis at 11mm downstream the nozzle is $5.1 \cdot 10^{15}$ atoms/cm^3 and this place very suits for the position of the skimmer with 0.6 mm orifice, because the Knudsen number in this case is about 1.2. It is interesting to note that at 11 mm distance from the nozzle the pressure on the jet axis (Fig. 7(a)) is 200 times less than background gas pressure. Whereas the gas density here (Fig. 7(b)) is twice as large as the background gas density outside the supersonic jet. One can see also from this figure that due to the supersonic gas expansion into vacuum the Mach number (Fig. 7(c)) in the jet is increased up to 36 and static temperature (Fig. 7(d)) drops below 1 K.
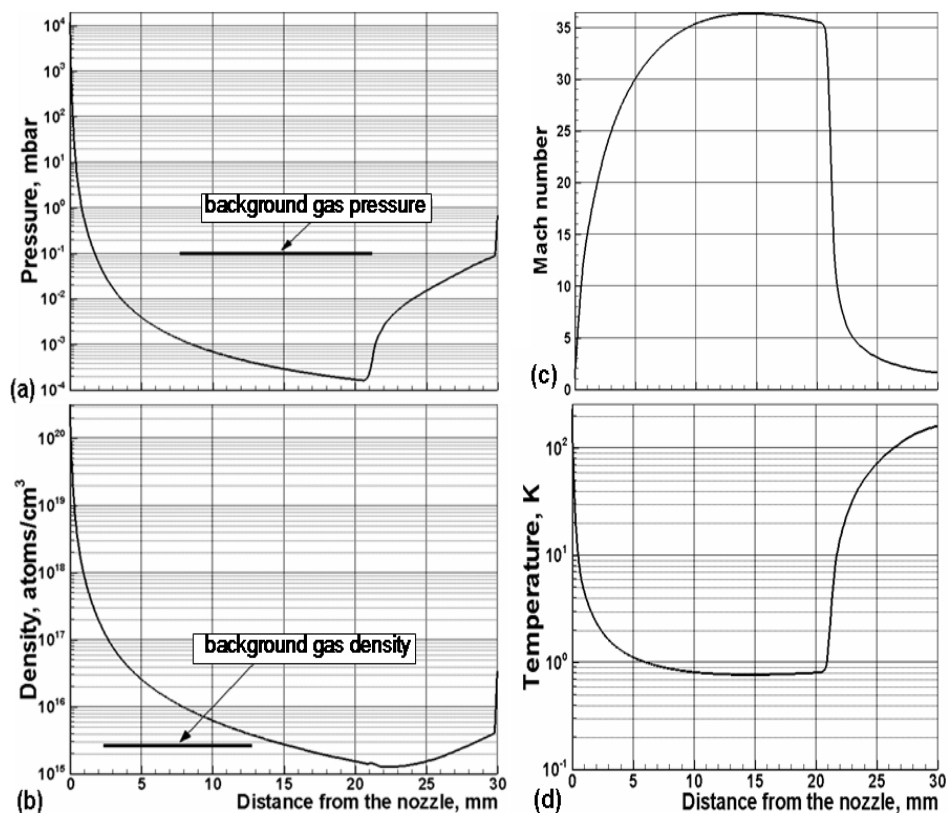
FIGURE 7. Calculated static pressure (a), density (b), Mach number (c) and static temperature (d) distributions along the axis for the same pulsed jet as that of Fig. 6.

Figure 8 shows radial profiles of the static pressure, density, static temperature and gas flow velocity at 11 mm downstream the nozzle. A strong barrel shock wave structure of the supersonic jet that is clear defined in the Figs.7 and 8 shields an axial jet region against background gas penetration into the gas-jet target and it is reasonable also to say that the nozzle-skimmer distance of about 11 mm looks as an optimum one.

Main design and operation parameters of the future gas-jet target apparatus for the case of the pulsed He supersonic jet are listed in the Table 2.
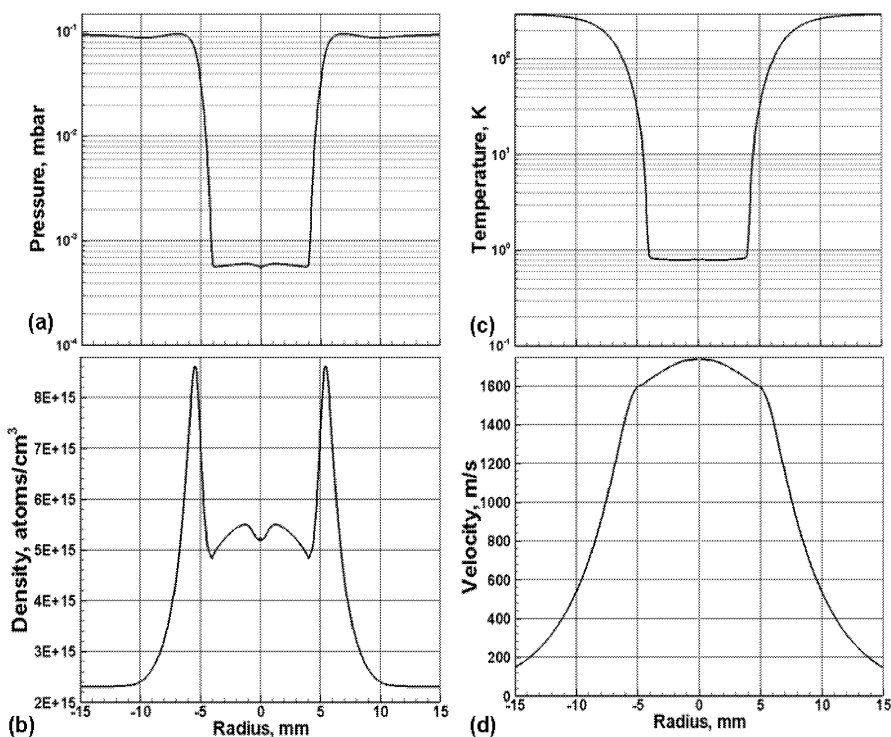
FIGURE 8. Calculated radial profiles of the static pressure (a), density (b), static temperature (c) and gas flow velocity (d) at 11 mm downstream the nozzle for the same pulsed jet as that of Figs. 6 and 7.

TABLE 2. Main design and operation parameters of the future gas-jet target apparatus for the case of pulsed He supersonic jet

Nozzle diameter	0.1 mm
1st skimmer diameter	0.6 mm
2nd skimmer diameter	2.2 mm
Nozzle-skimmer distance	11 mm
Skimmer-skimmer distance	25 mm
Skimmer-collimator distance	35 mm
Stagnation temperature	300 K
Stagnation pressure	22.6 bar
Gas flow rate though the nozzle during pulse	78.5 mbar·l/s
Beam temperature	0.78 K
Mach number	35.8
Beam velocity	1733 m/s
Target cross section	4 x 8 mm
Target-beam density	$3.0 \cdot 10^{13}$ atoms/cm^3

As seen from Table 2, the helium gas target of $3 \cdot 10^{13}$ atoms/cm^3 density will be accessible for atomic collision experiments with ultra slow antiproton beams. There can be no doubt that targets of other gases with similar densities will be possible here as well.

ACKNOWLEDGMENTS

REFERENCES

1. H.A. Torii, "Production of ultra-slow antiproton beams", Contribution to Workshop on Physics with Ultra Slow Antiproton Beams, RIKEN, March 2005 (in this book).
2. J. S. Cohen, Rep. Prog. Phys., **67**, 1769 (2004).
3. Z. Wang, "Development of an experimental apparatus for collisions between ultra-slow antiprotons and atoms/molecules" (internal report within the collaboration), January 2002.
4. K. Yoshiki Franzen, et al., "Transport beam line for ultraslow monoenergetic antiprotons", Rev. Sci. Instrum., **74**, 3305 (2003).
5. V. L. Varentsov, *Ph.D. Dissertation*, Leningrad Nuclear Physics Institute, 1986.
6. H. Reich, W. Bourgeois, B. Franzke, A. Kritzer, V. L. Varentsov, Nucl. Phys. **A 626**, 417 (1997).
7. O. Engels, et al., Hyperfine Interactions, **132**, 505(2001).
8. P. A. Lofy, *Ph.D. Dissertation*, Michigan State University, 2003.
9. A. N. Petunin, Uchenie zapiski TsAGI, vol. **7**, 112 (1976).
10. I. D. Boyd, P. F. Penko, D. L. Meissner, K. J. DeWitt, AIAA Jornal, **30**, 2453 (1992).
11. V. L. Varentsov, A. A. Inatiev, Nucl. Instr. And Meth., **A 413**, 447 (1998)
12. R. Burgei, et al., Nucl. Instr. And Meth., **204**, 53 (1982).
13. D. Anghinolfi, et al., Nucl. Instr. And Meth., **A 396**,23 (1997).
14. D. Allspach, et al., Nucl. Instr. And Meth., **A 410**,195 (1998).
15. N. Kuroda, et al., Phys. Rev. Lett., **94**, 023401 (2005).
16 O. F. Hagena, W. Obert,, J. Chem. Phys., **56**, 1793 (1972).
17 L. Abad, D. Bermejo, V.J. Herrero, J. Santos, Rev. Sci. Instrum, **66**, 3826 (1995).
18. Smith, R. A., T. Ditmire, J. W.G. Tisch, Rev. Sci. Instrum, **69**, 3799 (1998).
19. J. Libuda, I. Meusel, J. Hartmann, H.-J. Freund, Rev. Sci. Instrum, **71**, 4395 (2000).
20. S. Semushin, V. Malka, Rev. Sci. Instrum, **72**, 2961 (2001).
21. V. N. Popok, S. V. Prasalovich, M. Samuelsson, E. E. B. Campbell, Rev. Sci. Instrum, **71**, 4395 (2000).